IEEE Access
Multidisciplinary | Rapid Review | Open Access Journal

Received February 5, 2021, accepted February 17, 2021, date of publication February 19, 2021, date of current version March 1, 2021.

Digital Object Identifier 10.1109/ACCESS.2021.3060545

A Novel Thévenin Equivalent Model Considering the Correlation of Source-Grid-Load in Power Systems

PINGFENG YE[1], (Student Member, IEEE), XUESHAN HAN[1], MING YANG[1], (Senior Member, IEEE), YUMIN ZHANG[2], (Member, IEEE), YOUNAN PEI[1], AND XUAN ZHANG[2], (Student Member, IEEE)

[1]Key Laboratory of Power System Intelligent Dispatch and Control, Shandong University, Jinan 250061, China
[2]College of Electrical Engineering and Automation, Shandong University of Science and Technology, Qingdao 266590, China

Corresponding author: Xueshan Han (xshan@sdu.edu.cn)

This work was supported by the National Natural Science Foundation of China under Grant 51477091 and Grant 51407106.

ABSTRACT The coupled single-port circuit has been proposed for online voltage stability assessment based on wide-area measurements and grid equations. This circuit can explicitly reflect the influence of grid and load on voltage stability. However, it does not consider the impact of power generation. A novel Thévenin equivalent (TE) circuit considering the influence of source-grid-load on voltage stability is proposed in this paper. First, the impact of source-grid-load on the voltage of an individual load bus is divided into three parts according to the node-voltage equation. They are then decomposed into two components, respectively associated with the TE voltage and the TE impedance according to the TE circuit's characteristics. Finally, an online identification method for the parameters of the proposed TE circuit based on wide-area measurements is developed. Compared with the coupled single-port circuit, the proposed method has the advantage of being able to consider the influence of power generation on voltage stability and being consistent in form with traditional TE circuit without requiring approximation. Case studies on the IEEE 118-bus system illustrate the accuracy and effectiveness of the proposed method.

INDEX TERMS Correlation of source-grid-load, power system, parameter analysis, Thévenin equivalent, voltage stability.

NOMENCLATURE

Indices i	Index for buses.
j	Index for buses.
Parameters	
m	Number of generator buses.
n	Number of load buses.
k_{Pj}	Proportion of constant power load in load bus j.
k_{Zj}	Proportion of constant impedance load in load bus j.
K_{ij}	The $i-j$ element of network parameter matrix $\mathbf{K}$.
Z_{Li}	Equivalent load impedance of load bus i.
Z_{LLij}	The $i-j$ element of network parameter matrix $\mathbf{Z_{LL}}$.
Z_{LGGij}	The $i-j$ element of network parameter matrix $\mathbf{Z_{LGG}}$.
Z_{LGLij}	The $i-j$ element of network parameter matrix $\mathbf{Z_{LGL}}$.
$\mathbf{Y}$	Modified system admittance matrix after eliminating the tie buses.
Variables	
E_{Leq}	Equivalent voltage of DEL.
E_{Geq}	Equivalent voltage of DEG.
E_{LGeq}	Equivalent voltage of CELG.
$E_{Thev,i}$	TE voltage seen from load bus i.
I_{Li}	Current of load bus i.
I_{ZLj}	Current generated by the constant impedance load in load bus j.
I_{PLj}	Current generated by the constant power load in load bus j.
I_{Gj}	Current of generator bus j.
S_{Lj}	Apparent power of load bus j.

The associate editor coordinating the review of this manuscript and approving it for publication was Alex James.

V_{Li}	Voltage of load-bus i.
V_{Gj}	Voltage of generator bus j.
Z_{Leq}	Equivalent impedance of DEL.
Z_{Geq}	Equivalent impedance of DEG.
Z_{LGeq}	Equivalent impedance of CELG.
$Z_{Thev,i}$	TE impedance seen from load bus i.
ΔI_{Li}	Injection current compensated at load bus i.
$\mathbf{I_L}$, $\mathbf{V_L}$	Current and voltage vectors of load buses.
$\mathbf{V_L}$, $\mathbf{V_G}$	Current and voltage vectors of generator buses.
$\Delta I_{\mathbf{L}}$	Injection current vector of load buses.
$\Delta I_{\mathbf{G}}$	Injection current vector of generator buses.
$\Delta V_{\mathbf{L}}$	Voltage variation vector of load buses.
Subscript	
L, G	Represent load bus and generator bus, respectively.
"$i = 0$"	Load-bus i is open-circuited.
"$i = 1$"	Unit current is injected at load bus i.
Abbreviation	
CELG	Coupling effect of load buses and generator buses.
CPF	Continuation power flow.
DEG	Direct effect from generator buses.
DEL	Direct effect from load buses.
DVE	Direct voltage effect.
DVEC	Direct voltage effect component.
MBVSA	Measurement-based voltage stability assessment.
PMU	Phasor measurement unit.
TE	Thévenin equivalent.
VSA	Voltage stability assessment.

I. INTRODUCTION

Due to technical, economic, environmental concerns, the modern power system is operated at a high loading situation. As a result, voltage stability is closely related to power system security. With the increasing penetration of intermittent generations, additional reactive power compensation equipment is gradually replacing the voltage support role of synchronous generators [1]. Thus, the uncertainty and nonlinearity from intermittent generations, grid, loads with distributed generations are increasing. The uncertain and nonlinear factors from one bus will affect other buses' voltage stability [2]. The correlation of source-grid-load [3]–[5] is enhanced and will have a greater impact on the voltage stability of power systems [6]. Therefore, the voltage stability assessment (VSA) of power systems must consider the correlation of source-grid-load.

Traditionally, the VSA is performed with model-based approaches, such as time-domain simulations or continuation power flow (CPF) [7]. With the broad deployment of the phasor measurement units (PMUs), the measurement-based VSA (MBVSA) methods have attracted a lot of interest. One major category of MBVSA methods uses a Thévenin equivalent (TE) circuit to represent the entire power system seen from an individual load-bus. The TE includes a voltage source and an equivalent impedance, which can be estimated by local measurements [8]–[10]. Once the TE circuit is estimated, the voltage stability margin can also be evaluated according to the impedance match concept.

Despite its elegance, the impedance match (or the TE circuit) based MBVSA technique has some significant drawbacks. As discussed in [11], [12], one of its problems is the assumption that the TE parameters remain unchanged during the consecutive measurement windows. Such a requirement can hardly be satisfied during a voltage collapse process. Large-scale renewable energy integration has also affected its application under normal conditions. In addition to the drifting and time-varying problems of the parameters, [12] reveals that the technique also has some theoretical problems when applied to multi-load systems. Power system loads are nonlinear and dynamic. They cannot be simply represented as TE parameters for impedance match analysis. Furthermore, the technique cannot directly construct an analytical, quantitative relationship between the control measures and the TE parameters. Therefore, it is difficult to guide the optimization of preventive control. Despite many attempts and considerable progress [13]–[16], an improved technique that would entirely overcome all these problems has not been proposed. An online TE parameter identification method based on the wide-area measurements and the single state section has recently been proposed [17]. LU factorization is utilized to accelerate the calculation. Therefore, the method can quickly identify the TE parameters for the large power system. The technique can overcome the parameter drift problem based on the utilization of the node-voltage equation. However, the coupling effect from the nonlinearity and dynamics of loads is not considered in the method, which will reduce the accuracy and credibility of the VSA result.

A new method based on a coupled single-port circuit is proposed to overcome these difficulties [12], [18]. This method can overcome the parameter drift problem and indirectly form a quantitative mapping between control measures and the parameters, thus laying the foundation for subsequent preventive control. In the coupled single-port circuit, all the loads are brought outside of the equivalent system. Therefore, the coupling effects among the loads can be dealt with explicitly. The circuit can reveal the interactions of various loads in a power system and how such interactions affect the voltage stability margins of the individual load buses. Due to its advantages, the coupled single-port circuit is widely utilized in [19]–[22].

The coupled single-port circuit is obtained based on the derivation of the node-voltage equation, so its theoretical correctness is guaranteed. However, the circuit contains an additional impedance representing the coupling effects among the loads, which is different in form from the traditional TE circuit. Therefore, it cannot be used directly for the VSA. In order to maintain the formal consistency with the TE circuit, based on the coupled single-port circuit, three different approximate circuits are proposed and compared in [12]. However, none of the three circuits correlates the

voltage influence generated by the generator buses with the equivalent impedance. That is, the equivalent impedance does not contain information about the generator buses. In fact, the power injection mode of the system, which can be determined by the generator buses' state, will significantly impact the TE impedance [2]. As a simple example, when two generator buses provide active power regulation for a load bus, if the generator bus with a closer electrical distance to the load is dominant, the TE impedance seen from the load bus is relatively small, and vice versa. One of the three approximate circuits seems to have achieved acceptable results [12], but the effect of the power injection mode changes is not considered in its case studies. Unfortunately, as renewable energy power generation gradually replaces traditional generators, the power regulation mode or the participation factors of the generators will change more frequently. Therefore, this shortcoming of the coupled single-port circuit will greatly adversely impact its practical application.

Inspired by the concept of the coupled single-port circuit, this paper presents a novel TE circuit with analytical parameters. According to the node-voltage equation of the system, the influence of source-grid-load on the voltage of an individual load bus is divided into three parts. Then, they are decomposed into two components, respectively associated with the TE voltage and the TE impedance according to the characteristics of the TE circuit. Based on the proposed analytical TE circuit, a new online identification method for the TE parameters based on wide-area measurements is developed. Compared with the existing works, the novelties of this paper are as follows.

(1) A novel TE circuit is presented. Compared to the coupled single-port circuit, the proposed TE circuit has the advantage that it maintains formal consistency with the traditional TE circuit so that no further approximation is required. Furthermore, quantifiable connections between the TE parameters and the operation conditions of source-grid-load are also more clearly defined. Therefore, the accuracy of TE parameter identification and the VSA will be improved. Further analysis for preventive control can also be performed more efficiently.

(2) Based on the compensation method, a parameter identification method for the proposed TE circuit is presented. This method can simultaneously consider the influence of the changing characteristics of generations and loads on the TE parameters. Therefore, it is theoretically more accurate than the methods in [12] and [17] when the power injection mode fluctuates.

(3) The method in this paper can consider the influence of power generation on the TE parameters. Especially as the penetration rate of renewable energy power generation continues to increase, the method can be used to quantitatively analyze the influence of renewable energy change characteristics on the TE parameters.

The rest of the paper is organized as follows. In Section II, the coupled single-port circuit is introduced, TE parameters are analyzed, and a novel TE circuit considering the correlation of source-grid-load is proposed. Based on the compensation method, a parameter identification method for the proposed TE circuit is presented in Section III. Section IV discusses the related issues, including the factors affecting TE parameters and voltage interaction between load buses. Section V demonstrates and discusses the numerical results of the IEEE 118-bus system. Finally, Section VI concludes this paper.

II. PROPOSED THÉVENIN EQUIVALENT CIRCUIT

A. INTRODUCTION OF COUPLED SINGLE-PORT CIRCUIT

The buses in an interconnected grid can generally be classified into generator buses, load buses, and tie buses. Eliminating the tie buses, the node voltage equations can be expressed as [12]

$$\begin{bmatrix} -\mathbf{I_L} \\ \mathbf{I_G} \end{bmatrix} = [\mathbf{Y}] \begin{bmatrix} \mathbf{V_L} \\ \mathbf{V_G} \end{bmatrix} = \begin{bmatrix} \mathbf{Y_{LL}} & \mathbf{Y_{LG}} \\ \mathbf{Y_{GL}} & \mathbf{Y_{GG}} \end{bmatrix} \begin{bmatrix} \mathbf{V_L} \\ \mathbf{V_G} \end{bmatrix} \tag{1}$$

According to (1), the voltage vectors of load buses can be expressed as

$$\begin{aligned} \mathbf{V_L} &= \mathbf{K}\mathbf{V_G} - \mathbf{Z_{LL}}\mathbf{I_L} \\ \mathbf{Z_{LL}} &= \mathbf{Y_{LL}^{-1}} \\ \mathbf{K} &= -\mathbf{Y_{LL}^{-1}}\mathbf{Y_{LG}} \end{aligned} \tag{2}$$

From (2), for load-bus i, we can obtain

$$V_{Li} = \sum_{j=1}^{m} K_{ij} V_{Gj} - \sum_{j=1}^{n} Z_{LLij} I_{Lj} \tag{3}$$

The coupled single-port circuit corresponding to (3) is shown in Fig. 1.

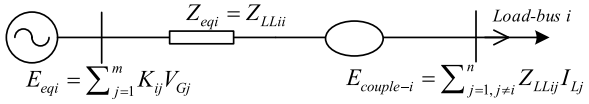

FIGURE 1. Coupled single-port system equivalent.

Compared to the traditional TE circuit, the difference is the new term $E_{couple-i}$ which represents the impact of other loads on bus i's equivalent circuit. Using this model, a power system can be broken down into a set of single-port circuits that have the impact of other loads included explicitly. However, this circuit is different in form from the traditional TE circuit. It cannot be used directly for the VSA. $E_{couple-i}$ contains both a portion of TE voltage and a portion of TE impedance, which is difficult to separate quantitatively. Therefore, it has to be approximated [12], [18], which leads to unavoidable errors.

B. ANALYSIS OF TE PARAMETERS

According to the TE circuit, the voltage of load-bus i can be expressed as

$$V_{Li} = E_{Thev,i} - Z_{Thev,i} I_{Li} \tag{4}$$

Both (3) and (4) can represent the voltage of a load bus. (3) contains more information about the system, so the coupled single-port circuit can be more convenient and detailed for further analysis than the TE circuit.

However, (3) only contains part of the information in (1). According to (1), the voltage vectors of generator buses can be expressed as

$$\mathbf{V_G} = \mathbf{Y_{GG}^{-1}I_G} - \mathbf{Y_{GG}^{-1}Y_{GL}V_L} \tag{5}$$

Substituting (5) into (2), the voltage vectors of load buses can also be expressed as

$$\begin{aligned} \mathbf{V_L} &= \mathbf{Z_{LGG}I_G} - \mathbf{Z_{LGL}I_L} \\ \mathbf{Z_{LGL}} &= [\mathbf{Y_{LL}} - \mathbf{Y_{LG}Y_{GG}^{-1}Y_{GL}}]^{-1} \\ \mathbf{Z_{LGG}} &= -\mathbf{Z_{LGL}Y_{LG}Y_{GG}^{-1}} \end{aligned} \tag{6}$$

It should be noted that if the line-to-ground admittance is ignored and there is no transformer in the system, $\mathbf{Z_{LGL}}$ does not exist. The reason is that a naturally established equation appears under this condition. That is, the sum of all generation currents is equal to the sum of all load currents. Therefore, if the current is selected as the state expression, the number of independent variables will be reduced by one, resulting in $[\mathbf{Y_{LL}} - \mathbf{Y_{LG}Y_{GG}^{-1}Y_{GL}}]$ not full rank. Fortunately, as long as there is a line-to-ground admittance or transformer branch, this will not happen.

From (6), for load-bus i, we can obtain

$$V_{Li} = \sum_{j=1}^{m} Z_{LGGij} I_{Gj} - \sum_{j=1}^{n} Z_{LGLij} I_{Lj} \tag{7}$$

Equations (3), (4), (7) depict the influence of the system's operation conditions on the voltage of load-bus i. Among them, (3) and (7) contain more details of the system. Therefore, they can be used to analyze the TE parameters in (4).

The four terms in (3) and (7) respectively represent different parts of the system's influence on V_{Li}.

Both $\sum_{j=1}^{m} K_{ij} V_{Gj}$ and $\sum_{j=1}^{m} Z_{LGGij} I_{Gj}$ reflect the influence associated with generator buses. The currents of generator buses are directly determined by the power injection mode of the system. The voltage amplitudes of the generator buses can be controlled to the reference values. However, according to the power flow, the voltage phase angles of the generator buses depend on the power injection mode, network, load of power systems. Therefore, $\sum_{j=1}^{m} Z_{LGGij} I_{Gj}$ can represent the direct influence from generator buses, and $\sum_{j=1}^{m} K_{ij} V_{Gj}$ can represent the total influence from generator buses.

Both $-\sum_{j=1}^{n} Z_{LLij} I_{Lj}$ and $-\sum_{j=1}^{n} Z_{LGLij} I_{Lj}$ reflect the system's influence associated with load currents. Comparing $-\sum_{j=1}^{n} Z_{LLij} I_{Lj}$ and $-\sum_{j=1}^{n} Z_{LGLij} I_{Lj}$, one can see that the coefficients are different. $\mathbf{Z_{LL}}(\mathbf{Y_{LL}^{-1}})$ only contains the network structure and parameters between load buses, and $\mathbf{Z_{LGL}}$ contains the network structure and line parameters among the load and generator buses. Therefore, $-\sum_{j=1}^{n} Z_{LLij} I_{Lj}$ only reflects the direct influence from load buses. $-\sum_{j=1}^{n} Z_{LGLij} I_{Lj}$ contains the influence from load buses and generator buses, which is directly related to the load currents.

When the load currents change, the transmission of the regulating currents from generator buses to load buses may affect V_{Li}. This effect depends on the power injection mode, structure, parameters of networks, as well as load mode of power systems, which is defined as the coupling effect of load buses and generator buses (CELG) in this paper. CELG on load-bus i can be reflected in $\sum_{j=1}^{m} K_{ij} V_{Gj}$ and $-\sum_{j=1}^{n} Z_{LLGij} I_{Gj}$, not in $-\sum_{j=1}^{n} Z_{LLij} I_{Lj}$ and $\sum_{j=1}^{m} Z_{LGGij} I_{Gj}$.

Based on the above discussion of (3) and (7), this paper divides the system's influence on the voltage of an individual load-bus into three parts:

1) The direct effect from load buses (DEL), which can be represented by $-\sum_{j=1}^{n} Z_{LLij} I_{Lj}$ in (3),
2) The direct effect from generator buses (DEG), which mainly reflects the direct effect from the power injection mode of the generator buses, and it can be represented by $\sum_{j=1}^{m} Z_{LGGij} I_{Gj}$ in (7),
3) CELG, whose expression can be obtained by the subtraction of (3) and (7) as follow

$$\sum_{j=1}^{m} K_{ij} V_{Gj} - \sum_{j=1}^{m} Z_{LGGij} I_{Gj} = -\sum_{j=1}^{n} (Z_{LGLij} - Z_{LLij}) I_{Lj} \tag{8}$$

where the left side of (8) represents the total influence from generator buses minus the DEG, and the right side represents the entire influence from load buses minus the DEL. Due to the certain balance of generator currents and load currents, both the left and right sides of (8) can represent the CELG.

Furthermore, the TE parameters can also reflect the system's influence on the voltage of an individual load-bus as shown in (4). Therefore, TE parameters can also be divided into three parts, which will be presented next.

C. DECOMPOSITION OF TE VOLTAGE AND TE IMPEDANCE

According to (4), the TE voltage's impact on V_{Li} does not change with I_{Li}. The TE impedance's effect on V_{Li} is shown as the voltage drop on the TE impedance, which will change with I_{Li}. Based on the characteristics of the TE circuit, the paper decomposes DEL, DEG, CELG into TE voltage and TE impedance, respectively.

According to Thévenin's theorem, the open-circuit voltage is equal to the TE voltage. Based on (3) and (7), the open-circuit voltage of load-bus i can be expressed as

$$V_{Li,i=0} = \sum_{j=1}^{m} K_{ij} V_{Gj,i=0} - \sum_{j=1}^{n} Z_{LLij} I_{Lj,i=0} \tag{9}$$

$$V_{Li,i=0} = \sum_{j=1}^{m} Z_{LGGij} I_{Gj,i=0} - \sum_{j=1}^{n} Z_{LGLij} I_{Lj,i=0} \tag{10}$$

Both (9) and (10) can represent the TE voltage seen from load bus i. According to (9), (10) and the analysis of the TE parameters, the TE voltage can also be divided into three parts as follows:

1) The equivalent voltage of DEL

$$E_{Leq,i} = -\sum_{j=1}^{n} Z_{LLij} I_{Lj,i=0} \tag{11}$$

It represents the part of DEL that is not affected by I_{Li}.

2) The equivalent voltage of DEG

$$E_{Geq,i} = \sum_{j=1}^{m} Z_{LGGij} I_{Gj,i=0} \tag{12}$$

It represents the part of DEG that is not affected by I_{Li}.

3) The equivalent voltage of CELG

$$E_{LGeq,i} = \sum_{j=1}^{m} K_{ij} V_{Gj,i=0} - \sum_{j=1}^{m} Z_{LGGij} I_{Gj,i=0}$$
$$or = -\sum_{j=1}^{n} (Z_{LGLij} - Z_{LLij}) I_{Lj,i=0} \quad (13)$$

It represents the part of CELG that is not affected by I_{Li}.

According to (9)-(13), the TE voltage seen from load bus i can be expressed as

$$E_{Thev,i} = V_{Li,i=0} = E_{Leq,i} + E_{Geq,i} + E_{LGeq,i} \quad (14)$$

Substituting for V_{Li} from (4) into (3) and (7), one has

$$E_{Thev,i} - Z_{Thev,i} I_{Li} = \sum_{j=1}^{m} K_{ij} V_{Gj} - \sum_{j=1}^{n} Z_{LLij} I_{Lj}$$
$$= \sum_{j=1}^{m} Z_{LGGij} I_{Gj} - \sum_{j=1}^{n} Z_{LGLij} I_{Lj} \quad (15)$$

Substituting for $E_{Thev,i}$ from (11)-(14) into (15), one has

$$Z_{Thev,i} = \frac{1}{I_{Li}} \left(\sum_{j=1}^{m} K_{ij} (V_{Gj,i=0} - V_{Gj}) - \sum_{j=1}^{n} Z_{LLij} (I_{Lj,i=0} - I_{Lj}) \right) \quad (16)$$

$$Z_{Thev,i} = \frac{1}{I_{Li}} \left(\sum_{j=1}^{m} Z_{LGGij} (I_{Gj,i=0} - I_{Gj}) - \sum_{j=1}^{n} Z_{LGLij} (I_{Lj,i=0} - I_{Lj}) \right) \quad (17)$$

According to (16), (17) and the analysis of the TE parameters, the TE impedance can also be divided into three parts as follows:

1) The equivalent impedance of DEL

$$Z_{Leq,i} = \frac{1}{I_{Li}} \sum_{j=1}^{n} Z_{LLij} (I_{Lj} - I_{Lj,i=0}) \quad (18)$$

It represents the part of DEL that changes with I_{Li}.

2) The equivalent impedance of DEG

$$Z_{Geq,i} = \frac{-1}{I_{Li}} \sum_{j=1}^{m} Z_{LGGij} (I_{Gj} - I_{Gj,i=0}) \quad (19)$$

It represents the part of DEG that changes with I_{Li}.

3) The equivalent impedance of CELG

$$Z_{LGeq,i} = \frac{1}{I_{Li}} \left(\sum_{j=1}^{m} K_{ij} (V_{Gj,i=0} - V_{Gj}) - \sum_{j=1}^{m} Z_{LGGij} (I_{Gj,i=0} - I_{Gj}) \right)$$
$$or = \frac{1}{I_{Li}} \sum_{j=1}^{n} [(Z_{LGLij} - Z_{LLij})(I_{Lj} - I_{Lj,i=0})] \quad (20)$$

It represents the part of CELG that changes with I_{Li}.

According to (16)-(20), the TE impedance seen from load bus i can be expressed as

$$Z_{Thev,i} = Z_{Leq,i} + Z_{Geq,i} + Z_{LGeq,i} \quad (21)$$

Based on the analytical expression of the TE voltage (14) and TE impedance (21), this paper presents a novel TE circuit with analytical parameters, as shown in Fig. 2.

Compared to the traditional TE circuit, the proposed TE circuit form a quantitative mapping between the system's operation conditions and the TE parameters, thus laying the foundation for subsequent analysis and preventive control.

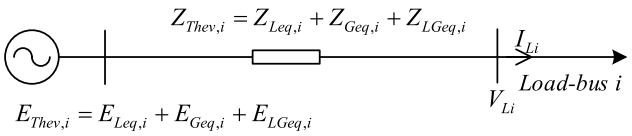

FIGURE 2. The proposed Thevenin equivalent circuit.

Compared to the coupled single-port circuit, the proposed TE circuit has the advantage that it maintains formal consistency with the traditional TE circuit, so that no further approximation is required.

III. IDENTIFICATION OF THÉVENIN EQUIVALENT PARAMETERS

According to (11)–(13) and (18)–(20), the key to identifying the parameters of the proposed TE circuit is to obtain the currents of load buses and generator buses when the assessed load bus is open-circuited.

Under the wide-area measurement condition, [17] proposes a method that can quickly identify the TE parameters of large power grids based on the compensation method. To avoid repetitive Gaussian elimination of the high-dimensional linear system, lower upper factorization and optimized substitution are used to accelerate the open-circuit voltage solution process. Based on [17], a method to identify the parameters of the proposed TE circuit is presented. The main difference between the proposed method and method [17] is that the method in this paper identifies the parameters of the proposed TE circuit, while [17] identifies the parameters of the traditional TE circuit. Meanwhile, the proposed method considers the changing characteristics of load and generation, which are not considered in [17].

Taking load bus i as an example, an injection current ΔI_{Li} is compensated at bus i, so that the injection current from system to load bus i is zero, which is equivalent to open load bus i, as shown in Fig. 3.

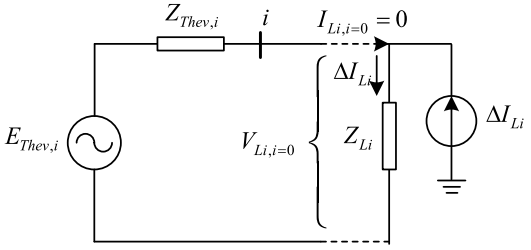

FIGURE 3. TE circuit seen from load bus i using compensation method.

The current and voltage of the bus can be obtained by measurement. Therefore, the key for the identification is to calculate the influence of ΔI_{Li} on the voltage and current of each bus.

The unit current is injected at load bus i, and the injection current of other load buses is zero. In order to ensure the balance of the system current, the generator buses adjust the injection current according to the participation factor, and the injection current vector of the load buses can be denoted as $\Delta\mathbf{I}^{\mathbf{1}}_{\mathbf{L,i=1}} = [0, \cdots -1, \cdots 0]^T$. The injection current vector of generator buses is denoted as $\Delta\mathbf{I}_{\mathbf{G,i=1^1}} = [F_1, \cdots F_j, \cdots F_m]^T$, where F_j is the participation factor of generator bus j, and $\sum_{j=1}^{m} F_j = 1$. By substituting the injection current vector into (1), the voltage variation vector of load buses $\Delta\mathbf{V}_{\mathbf{L,i=1^1}}$ caused by the injection current can be calculated. Since the bus admittance matrix is invariant in each bus's parameter identification process, LU factorization can be utilized to accelerate this calculation. For specific details of LU factorization, please refer to [17].

Considering the load characteristics, the current of the load bus will change with the voltage, and then the injection current vector of load buses will become:

$$\begin{aligned}\Delta\mathbf{I}_{\mathbf{L,i=1^2}} &= -[\frac{\mathrm{d}I_{L1}}{\mathrm{d}I_{Li}}, \cdots, \frac{\mathrm{d}I_{Li-1}}{\mathrm{d}I_{Li}}, 1, \cdots, \frac{\mathrm{d}I_{Ln}}{\mathrm{d}I_{Li}}]^T \\ &= -[\frac{\mathrm{d}I_{L1}}{\mathrm{d}V_{L1}} \cdot \frac{\mathrm{d}V_{L1}}{\mathrm{d}I_{Li}}, \cdots, \frac{\mathrm{d}I_{Li-1}}{\mathrm{d}V_{Li-1}} \cdot \frac{\mathrm{d}V_{Li-1}}{\mathrm{d}I_{Li}}, \\ &\quad 1, \cdots, \frac{\mathrm{d}I_{Ln}}{\mathrm{d}V_{Ln}} \cdot \frac{\mathrm{d}V_{Ln}}{\mathrm{d}I_{Li}}]^T \end{aligned} \tag{22}$$

where $\mathrm{d}I_{Li-1}/\mathrm{d}I_{Li}$ represents the current change of load bus $i-1$ after the unit current is injected into load bus i. $\mathrm{d}I_{Li-1}/\mathrm{d}V_{Li-1}$ is determined by the load characteristics. $-\mathrm{d}V_{Li-1}/\mathrm{d}I_{Li}$ can be represented by the i-1th element of $\Delta\mathbf{V}_{\mathbf{L,i=1^1}}$

The load characteristics are determined by the load modeling. Due to the development of synchronized phasor measurement technologies, some load modeling methods based on local measurement have been proposed [23], [24]. Depending on the application scenarios, different static and dynamic load models are used in those methods. The ZIP model can be adopted in static voltage stability analysis as an example [2], [24]. Then, when the voltage change of load bus j is $\Delta\mathbf{V}_{\mathbf{Lj,i=1^1}}$, its current change can be expressed as

$$\begin{aligned}\Delta I_{Lj,i=1^2} &= \frac{dI_{Lj}}{dV_j} \cdot \Delta V_{Lj,i=1^1} = (\frac{dI_{ZLj}}{dV_j} + \frac{dI_{PLj}}{dV_j}) \cdot \Delta V_{Lj,i=1^1} \\ &= (\frac{[k_{Zj}S_{Lj}]^*}{V_{Lj}^2} - \left[\frac{k_{Pj}S_{Lj}}{V_{Lj}^2}\right]^*) \cdot \Delta V_{Lj,i=1^1} \end{aligned} \tag{23}$$

Substituting for $\mathrm{d}I_{Lj}/\mathrm{d}V_{Lj}$ from (23) into (22), the updated injection current vector $\Delta\mathbf{V}_{\mathbf{L,i=1^2}}$ considering power injection mode and the load characteristics can be formulated. In order to ensure current balance, the current vector of generator buses should be updated to $\Delta\mathbf{I}_{\mathbf{G,i=1^2}} = \Delta\mathbf{I}_{\mathbf{G,i=1^1}} \cdot \sum_{j=1}^{n} \Delta\mathbf{I}_{\mathbf{Lj,i=1^2}}$. The update process can continue until the accuracy requirement is reached. In the simulations of this paper, the number of iteration k is taken as 4.

After k updates, $\Delta\mathbf{I}_{\mathbf{L,i=1^k}}$, $\Delta\mathbf{I}_{\mathbf{G,i=1^k}}$ and $\Delta\mathbf{V}_{\mathbf{L,i=1^k}}$ are the final results. According to the equivalent circuit shown in Fig. 3, one can get

$$V_{Li,i=0} = \Delta I_{Li} Z_{Li} \tag{24}$$

Based on the superposition principle and the compensation method, the open-circuit voltage of load bus i can be expressed as

$$V_{Li,i=0} = V_{Li} + \Delta V_{Li} = V_{Li} + \Delta I_{Li} \cdot \Delta V_{Li,i=1^k} \tag{25}$$

Combining (24) and (25), one has

$$\Delta I_{Li} = \frac{V_{Li}}{Z_{Li} - \Delta V_{Li,i=1^k}} \tag{26}$$

When load bus i is open-circuited, the current vectors of load buses and generator buses are

$$\mathbf{I}_{\mathbf{L,i=0}} = \mathbf{I}_{\mathbf{L}} + \Delta I_{Li} \cdot \Delta\mathbf{I}_{\mathbf{L,i=1^k}} \tag{27}$$

$$\mathbf{I}_{\mathbf{G,i=0}} = \mathbf{I}_{\mathbf{G}} + \Delta I_{Li} \cdot \Delta\mathbf{I}_{\mathbf{G,i=1^k}} \tag{28}$$

where, $\mathbf{I}_{\mathbf{L}}$ and $\mathbf{I}_{\mathbf{G}}$ are measurement current vectors of load buses and generator buses, respectively.

Then, according to (11)–(14) and (18)–(21), TE voltage, TE impedance, and their three components can be calculated. The flowchart of the proposed method is shown in Fig. 4.

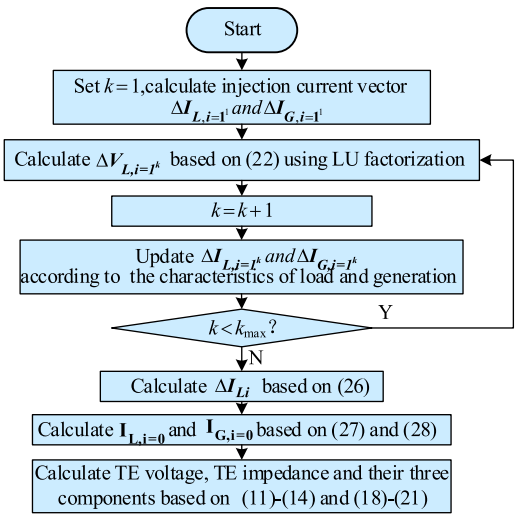

FIGURE 4. Flowchart of the method to identify the parameters of the proposed TE circuit.

IV. DISCUSSION AND ANALYSIS OF RELEVANT ISSUES

A. THE FACTORS AFFECTING TE PARAMETERS

TE voltage and TE impedance are respectively divided into three parts in the proposed TE circuit, as shown in Fig. 2. They are mainly affected by three factors: voltage support structure, power injection mode, and load characteristics.

The voltage support structure of power systems is determined by the structure and parameters of the network and buses' attributes (generator buses or load buses). It determines the relevant network parameter matrixes in (11)–(13) and (18)–(20). For example, a generator bus will become a load bus if its power capacity limit is reached.

Power injection mode of power system determines currents of generator buses and their regulations, which mainly influence the equivalent voltage and impedance of DEG, as well as the equivalent voltage and impedance of CELG according to (12), (13), (19), (20).

Load characteristics are critical to the accuracy of voltage stability analysis [2]. They will influence the changes in load currents when the bus under study is open-circuited. Therefore, they can affect the equivalent voltage and impedance of DEL, as well as the equivalent voltage and impedance of CELG according to (11), (13), (18), (20). For example, if the currents of all load buses are constant, then $I_{Lj} = I_{Lj,i=0}$ $(i \neq j)$, the equivalent impedances of DEL and CELG from other load buses will be zero according to (18) and (20). That means other loads will not affect the TE impedance of an individual bus if the currents of load buses are all constant.

B. VOLTAGE INFLUENCE BETWEEN LOAD BUSES

DEL embodies the direct voltage effect (DVE) between load buses. CELG reflects the voltage variations caused by the transfer of the regulated power and current from generator buses to load buses. Next, their specific performances are analyzed through a 5-bus system, as shown in Fig. 5. Bus 1 and bus 5 are generator buses, bus 2, bus 3, bus 4 are load buses. Z_{12} and Z_{23} are the impedances of line 1-2 and line 2-3, respectively.

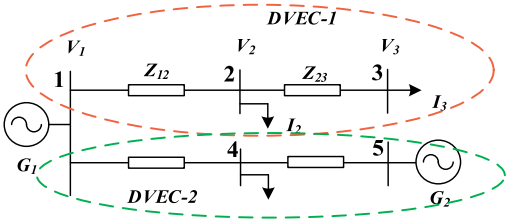

FIGURE 5. 5-bus system.

If the voltage of bus 2 changes ΔV_2, the load current at bus 3 is required to be constant, and the transmission current on line 2-3 is $I_{2,3} = (V_2 - V_3)/Z_{23}$. Its full differential expression is $d\dot{I}_{2,3} = z_{23}^{-1}\left(d\dot{V}_2 - d\dot{V}_3\right)$. To keep the current transmitted to bus 3 unchanged, which means $dI_{2,3} = 0$, the voltage variation at bus 3 ΔV_3 must be equal to ΔV_2.

If the voltage at bus 3 changes $\Delta V3$, the load current at bus 2 is required to be constant, the variation of transmission current on line 2-3 is $\Delta\dot{I}_{2,3} = z_{23}^{-1}\left(\Delta\dot{V}_2 - \Delta\dot{V}_3\right)$, the variation current of line 1-2 is $\Delta\dot{I}_{1,2} = -z_{12}^{-1}\Delta\dot{V}_2$. To keep the current of bus 2 unchanged, $\Delta I_{1,2} = \Delta I_{2,3}$ must be satisfied, thus $\Delta V_2 = \Delta V_3 Z_{12} Z_{23}/(Z_{12} + Z_{23})$.

The performance of DVE among the load buses of power systems is similar to the interaction of particle positions in a vertical suspension elastic system. When the position of a particle (analog voltage) is shifted, all non-fixed particles connected to that particle will be shifted despite their constant weight (analog load power or current).

The influence of DVE between buses can be transmitted continuously through the lines, but the voltage amplitudes of generator buses (PV buses) are controlled as reference values. Therefore, if all the connecting paths between two load buses need to pass through generator buses, there will be no DVE between them. In this paper, a connected network, whose load buses all have DVE between each other, is called a DVE component (DVEC) of the power system.

Different DVECs are isolated by generator buses. By removing all generator buses from the grid and analyzing the remaining grid connectivity through a search algorithm, the grid can be decomposed by DVECs.

For the 5-bus system shown in Fig. 5, bus 1 divides the system into 2 DVECs. There is no DEC between bus 4 and bus 2, bus 4 and bus 3.

There is no DVE between load buses in different DVECs, but this does not limit the voltage effect caused by the transfer of the regulated power and current.

For the system of Fig. 5, if the generators of bus 1 and bus 5 are both involved in active power regulation, then when the demand of bus 2 changes, the voltage of bus 4 will be affected by the transmission of the regulated power from bus 5. But in turn, the change in the demand of bus 4 does not affect the voltage of bus 2.

In summary, DVE causes the voltage variations to diffuse among the load buses of a DVEC fully. CELG causes the voltage variations to spread among different DVECs.

V. CASE STUDY

A. ACCURACY VERIFICATION

The accuracy of the proposed method is tested on the IEEE 118-bus system. The system parameters can be found in [25]. The power flow result under the test system data given by MATPOWER [26] is used as the initial state section.

Firstly, three pairs of TE parameters of bus 84 are calculated according to the proposed method, method [17], and method [12], respectively. According to the calculated TE parameters, 3 different two-bus equivalent systems can be obtained.

Then, increase the load of bus 84 by 2% of the initial load, and keep the load of other buses unchanged. Substituting the increased load of bus 84 into the two-bus equivalent systems to perform power flow calculation, and take the voltage amplitudes at bus 84 as the calculated values. The power flow calculation is performed on the 118-bus system, and the voltage amplitude of bus 84 is obtained as the baseline value. According to the new state section of the 118-bus system, the three pairs of TE parameters are updated according to the proposed method, method [17], and method [12].

Then, continue to add 2% of the original load to bus 84, and repeat the above steps 100 times. That is, the CPF calculation is performed using the 118-bus system and the 3 two-bus equivalent systems, respectively. The difference is that the system parameters of the 118-bus system remain unchanged, while the two-bus equivalent systems need to update the TE parameters for each calculation step.

CPF is widely used in VSA due to its simple and clear principles. The disadvantage is the heavy computational burden. The more accurate the TE parameters, the CPF curves obtained by the simulation of the two-bus equivalent systems should be closer to the CPF curve obtained by the 118-bus system. The comparison results are shown in Fig. 6.

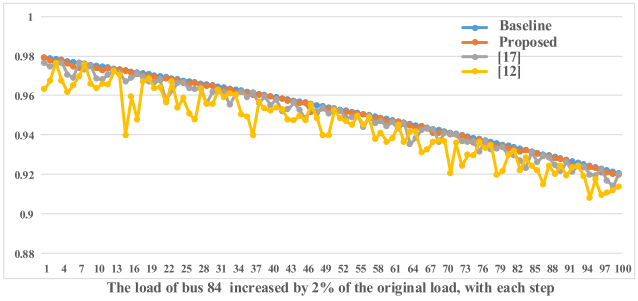

FIGURE 6. Comparison results of CPF curves at bus 84.

Fig. 6 shows that the accuracy of the TE parameters calculated by the proposed method is higher than those of method [17] and method [12]. Compared with the baseline values of CPF curve, the average error of the proposed method is 0.184%, and the maximum error is 0.351%. The average errors of method [17] and method [12] are 0.861% and 1.293%, and the maximum errors are 2.838% and 3.199%, respectively.

The simulation is computed using MATLAB running on a computer with 16G RAM and Intel i5-9300H CPU. The average calculation times for the proposed method, method [17], and method [12] are 153 ms, 121 ms, and 470 ms, respectively. LU factorization in [17] is introduced into the method. Although the proposed method has more steps, the most time-consuming LU factorization only needs to be performed once. In principle, the proposed method is only slightly slower than the method in [17], and the speed of the method [17] is its advantage.

B. EFFECTIVENESS VERIFICATION

Compared to the traditional TE circuit, the parameters of the proposed TE circuit have three components and contain more system information from the node-voltage equation. Therefore, it can be used for more detailed analysis.

IEEE 118-bus system is taken as the test system. 54 generator buses divide the 118-bus system into 26 DVECs, among which 13 DVECs only have one load bus. Fig. 7 shows the largest DVEC and a DVEC with a single load bus in the 118-bus system. Increase the power of all loads in Fig. 7 with a constant power factor until the system reaches static voltage instability. The impedance modulus margin index of bus 84 first reaches 1, so bus 84 is the key bus to the voltage stability of the system.

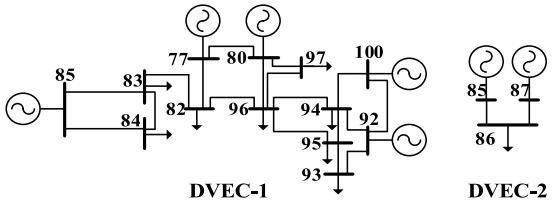

FIGURE 7. Two DVECs of IEEE 118-bus system.

In order to clearly reflect the variation pattern of the TE parameters of bus 84 with increasing loads, the TE parameters obtained by the proposed method, and their three components, are represented by polar plots.

TE voltage and TE impedance of bus 84 as loads increase are shown in Fig. 8. Fig. 9 shows equivalent voltages and impedances of DEL, DEG, CELG at bus 84 as the loads increase. The blue vector clusters represent the corresponding equivalent voltage and impedance vectors as the loads gradually increase, and the broken lines represent the direction of change.

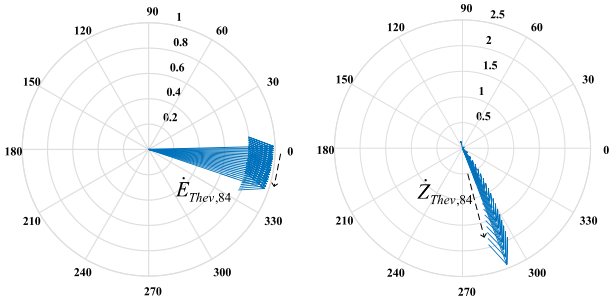

FIGURE 8. TE Voltage and TE impedance of bus-84 as loads increase.

Fig. 8 shows that as loads increase, the TE voltage's phase angle gradually decreases, the amplitude changes little, and the amplitude of TE impedance increases significantly. It can be seen from Fig. 9 that the equivalent voltage of DEG has the largest amplitude, followed by the equivalent voltage of CELG, while the equivalent voltage of DEL is relatively small. The equivalent voltage of CELG weakens the equivalent voltage of DEG in the vertical direction ($\pm 90°$), and the weakening component increases with the increase of loads. The equivalent voltage of DEL weakens the equivalent voltage of DEG in the horizontal direction ($\pm 0°$), and the weakening component also increases with the increase of loads.

Among the equivalent impedances, the amplitude of DEG is also the largest, followed by CELG, and DEL is the smallest. If a load bus is closer to the generator buses that provide regulated power, then when the load changes, the transmission of regulated power will have less effect on its voltage. This means that the TE impedance is relatively small. Otherwise, the TE will be relatively large. Therefore, the generator buses will have a more significant impact on the TE impedance.

In order to analyze the effect of other load buses on the voltage of bus 84, Fig. 10 and Fig. 11 show the influence of bus 86 and bus 96 on the TE parameters at bus 84 as loads increase.

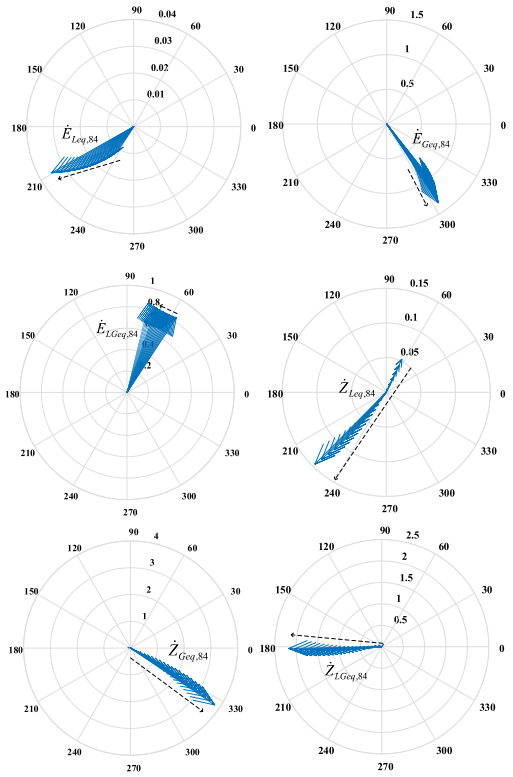

FIGURE 9. Equivalent voltages and impedances of DEL, DEG and CELG at bus 84 as loads increase.

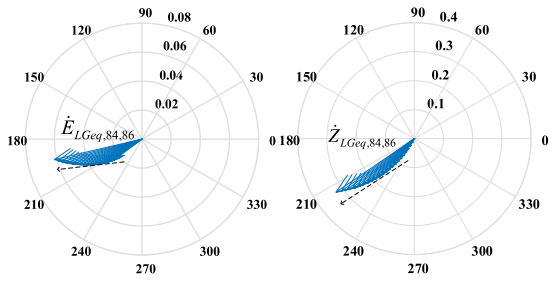

FIGURE 10. Equivalent voltage and impedance of DEL from bus 86 on bus 84.

The equivalent voltage and impedance of DEL from bus 86 on bus 84 are shown in Fig. 10. Bus 86 and bus 84 are located in different DVECs, and there is no DVE between the two load buses. Therefore, bus 86 does not generate equivalent voltage and impedance at bus 84. However, the regulated power transmission of bus 86 will affect the voltage of the load bus in DVEC-1 so that it will produce equivalent voltage and impedance of CELG at bus 84. Compared to Fig. 10 with Fig. 7, one can be seen that as loads increase, bus 86 will generally reduce the TE voltage and increase the TE impedance at bus 84. Both will facilitate the maximum power transfer from the system to bus 84 and reduce its voltage stability margin.

The equivalent voltage and impedance of DEL and CELG from bus 96 on bus 84 are shown in Fig. 11. Bus 96 and bus 84 are located in the same DVEC, so bus 96 will generate

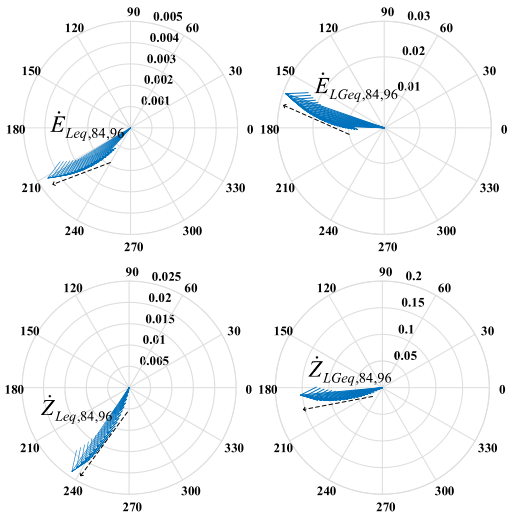

FIGURE 11. Equivalent voltage and impedance of DEL and CELG from bus 96 on bus 84.

equivalent voltages and impedances of DEL and CELG at bus 84. Comparing Fig. 11 with Fig. 7, it can be seen that, as loads increase, the equivalent voltage and impedance generated by bus 96 generally decrease the TE voltage and increase the TE impedance at bus 84. Therefore, the maximum power transfer to bus 84 and its voltage stability margin will be reduced.

When a bus reaches the maximum power point, some researchers believe that the system as a whole will also reach the maximum power transfer point, that is, all load buses can no longer increase the load. In fact, this conclusion is not consistently correct.

In this example, both bus 96 and bus 86 will produce equivalent voltage and impedance at bus 84. According to the previous simulation conclusion, when bus 84 reaches the maximum power point, if bus 96 or bus 86 increases the load, it will reduce the maximum transfer power to bus 84, so bus 96 and bus 86 cannot really increase the load. However, bus 86 is at DVEC-2, and there is no DVE between it and DVEC-1. At the same time, the load buses in DVEC-1 also have no CELG with bus 86. Therefore, when bus 86 reaches the maximum power point, the load buses in DVEC-1 can still increase the loads, which does not affect the TE parameters at bus 86.

C. INFLUENCE OF INTERMITTENT DISTRIBUTED GENERATION

Compared with the existing TE circuit, the biggest advantage of the proposed method is that it can explicitly reflect the influence of power generation changes on TE parameters and voltage stability. When the penetration ratio of intermittent power generation continues to increase, the advantages of this method will become more obvious. To analyze the influence of intermittent distributed generation on TE parameters, two wind farms with unit constant power factor control and rated

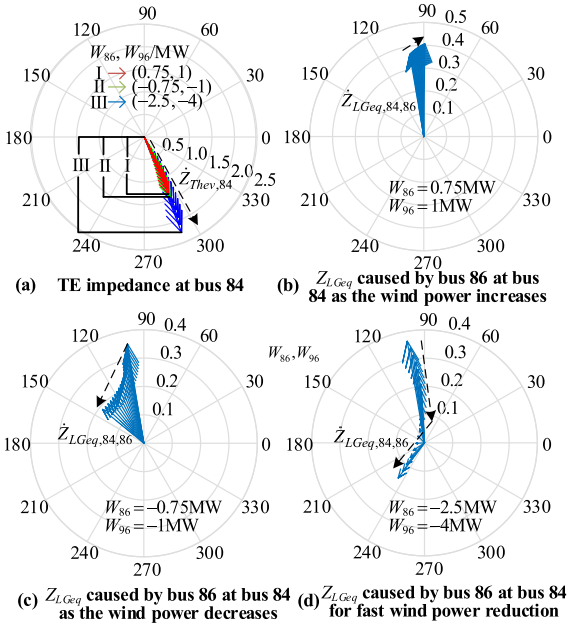

(a) TE impedance at bus 84 (b) Z_{LGeq} caused by bus 86 at bus 84 as the wind power increases

(c) Z_{LGeq} caused by bus 86 at bus 84 as the wind power decreases (d) Z_{LGeq} caused by bus 86 at bus 84 for fast wind power reduction

FIGURE 12. The TE impedance at bus 84 and the equivalent impedance of CEGL produced by bus 86 on bus 84 as loads increase.

capacity of 45 MW are connected to bus 86 and bus 96 of the IEEE 118-bus system. Let their output power at the initial point be 25 MW and 32 MW, respectively.

Increase all loads with a constant power factor until the system reaches static voltage instability. Unlike traditional sources, the output of wind power is highly uncertain and cannot be controlled entirely. To analyze the influence of wind power changes on TE parameters, let (W86, W96) be the output variations of the two wind farms when the load power increases by 10%, and take 3 pairs of values (0.75, 1) MW, (−0.75, −1) MW, (−2.5, −4) MW.

Fig. 12 shows the TE impedance at bus 84 and the equivalent impedance of CEGL produced by bus 86 on bus 84 as the load increase. It can be seen from Fig. 12-(a) that if the wind power output increases with the loads, the amplitude of TE impedance at bus 84 increases slowly, which is represented by vector cluster I. However, when the wind power output decreases with the increase of loads, the amplitude increases with the increase of the wind power change rate, as shown by vector the clusters II and III.

It can be seen from (b), (c), (d) of Fig. 12 that after bus 86 is connected to wind power, the equivalent impedance of CEGL produced by bus 86 on bus 84 reduces the TE impedance amplitude at bus 84, which is beneficial to the static voltage stability of bus 84. If the wind power increases as the load increase, bus 86 can further help reduce the TE impedance amplitude at bus 84, as shown in Fig. 12-(b). If the wind power decreases as loads increase, the positive effect of bus 86 on the voltage stability of bus 84 continues to weaken, as shown in Figure 12-(c). When the wind power decreases faster, the positive effect of bus 86 on the voltage stability of bus 84 also weakens more quickly. When wind power is less than the load of bus 86, the equivalent impedance of CELG produced by bus 86 on bus 84 will increase the TE impedance amplitude at bus 84, which will reduce its static voltage stability, as shown in Figure 12-(d).

Based on the above analysis, it can be concluded that different power variations of intermittent distributed generations will have significantly different effects on the TE parameters.

VI. CONCLUSION

The voltage stability of power systems will change with the operating conditions of power generation, grid and load. Therefore, when power generation, grid, or load changes during operation, if the identified Thévenin equivalent (TE) parameters do not change accordingly, errors will occur in the voltage stability assessment (VSA) based on the TE circuit. However, the existing TE circuit cannot explicitly reflect the influence of power generation on TE parameters. This paper proposes a novel TE circuit considering the impact of source-grid-load on voltage stability. The quantifiable connections between the TE parameters and the conditions of source-grid-load are explicitly defined. Under the wide-area measurement condition, the proposed TE circuit can quickly and explicitly reflect changes in power generation, grid, and load. As the penetration ratio of renewable energy generation continues to increase, the frequency and magnitude of power generation changes will continue to increase, and the advantages of the proposed method will become more and more prominent.

The numerical results on the IEEE 118-bus system show that the variation of intermittent power generation will have a significant impact on the TE parameters. Therefore, the influence of power generation uncertainty on voltage stability should be considered in the VSA based on the TE circuit. Our future work will incorporate the uncertainty of non-distributable renewable energy into the proposed TE analytical circuit, and identify the voltage stability problems caused by the uncertainty based on the proposed method.

REFERENCES

[1] B. B. Adetokun, C. M. Muriithi, and J. O. Ojo, "Voltage stability assessment and enhancement of power grid with increasing wind energy penetration," *Int. J. Electr. Power Energy Syst.*, vol. 120, Sep. 2020, Art. no. 105988.

[2] H. Liu, J. Su, J. Qi, N. Wang, and C. Li, "Decentralized voltage and power control of multi-machine power systems with global asymptotic stability," *IEEE Access*, vol. 7, pp. 14273–14282, 2019.

[3] D. Shuai, Z. Qianfan, Z. Weipan, Z. Chaowei, and N. Tuopu, "A compound control strategy for improving the dynamic characteristics of the DC-link voltage for the PMSM drive system based on the quasi-Z-source inverter," *IEEE Access*, vol. 7, pp. 151929–151938, 2019.

[4] A. Adib, B. Mirafzal, X. Wang, and F. Blaabjerg, "On stability of voltage source inverters in weak grids," *IEEE Access*, vol. 6, pp. 4427–4439, 2018.

[5] H. Li, H. Liu, Y. Yuan, and Q. Zhou, "Large-scale source-grid-load friendly interactive system introduction and real load shedding verification test technology," *J. Eng.*, vol. 2019, no. 16, pp. 2649–2653, Mar. 2019.

[6] Y. Yang, S. Lin, Q. Wang, Y. Xie, and M. Liu, "Multi-objective optimal control approach for static voltage stability of power system considering interval uncertainty of the wind farm output," *IEEE Access*, vol. 8, pp. 119221–119235, 2020.

[7] A. S. Matveev, J. E. Machado, R. Ortega, J. Schiffer, and A. Pyrkin, "A tool for analysis of existence of equilibria and voltage stability in power systems with constant power loads," *IEEE Trans. Autom. Control*, vol. 65, no. 11, pp. 4726–4740, Nov. 2020.

[8] X. Liang, M. N. S. K. Shabbir, N. Khan, and X. Yan, "Measurement-based characteristic curves for voltage stability and control at the point of interconnection of wind power plants," *Can. J. Electr. Comput. Eng.*, vol. 42, no. 3, pp. 163–172, 2019.
[9] Y. Zhang, Y. Xu, R. Zhang, and Z. Y. Dong, "A missing-data tolerant method for data-driven short-term voltage stability assessment of power systems," *IEEE Trans. Smart Grid*, vol. 10, no. 5, pp. 5663–5674, Sep. 2019.
[10] H.-N. Hsun, J.-H. Liu, J.-S. Cheng, and X.-B. Jiang, "Measurement-based voltage stability assessment by augmented coupled single-port models considering wind power generators," in *Proc. IEEE 2nd Int. Conf. Power Energy Appl. (ICPEA)*, Singapore, Apr. 2019, pp. 202–206.
[11] Y. Wang, W. Li, and J. Lu, "A new node voltage stability index based on local voltage phasors," *Electr. Power Syst. Res.*, vol. 79, no. 1, pp. 265–271, Jan. 2009.
[12] Y. Wang, I. R. Pordanjani, W. Li, W. Xu, T. Chen, E. Vaahedi, and J. Gurney, "Voltage stability monitoring based on the concept of coupled single-port circuit," *IEEE Trans. Power Syst.*, vol. 26, no. 4, pp. 2154–2163, Nov. 2011.
[13] J. Zhao, Z. Wang, C. Chen, and G. Zhang, "Robust voltage instability predictor," *IEEE Trans. Power Syst.*, vol. 32, no. 2, pp. 1578–1579, Mar. 2017.
[14] J. Chen, M. Fasehulla, S. Tan, and W. Yu, "Robust voltage regulation if unmanned electric vehicles," in *Proc. 3rd Int. Symp. Auto. Syst. (ISAS)*, Shanghai, China, May 2019, pp. 249–254.
[15] A. R. R. Matavalam and V. Ajjarapu, "PMU-based monitoring and mitigation of delayed voltage recovery using admittances," *IEEE Trans. Power Syst.*, vol. 34, no. 6, pp. 4451–4463, Nov. 2019.
[16] A. R. Matavalam and V. Ajjarapu, "Sensitivity based Thevenin index with systematic inclusion of reactive power limits," in *Proc. IEEE Power Energy Soc. Gen. Meeting (PESGM)*, Portland, OR, USA, Aug. 2018, p. 1.
[17] Z. Yun, X. Cui, and K. Ma, "Online Thevenin equivalent parameter identification method of large power grids using LU factorization," *IEEE Trans. Power Syst.*, vol. 34, no. 6, pp. 4464–4475, Nov. 2019.
[18] W. Li, "Investigation on the Thevenin equivalent parameters for online estimation of maximum power transfer limits," *IET Gener., Transmiss. Distrib.*, vol. 4, no. 10, pp. 1180–1187, 2010.
[19] C. Liu, F. Hu, D. Shi, X. Zhang, K. Sun, and Z. Wang, "Measurement-based voltage stability assessment considering generator VAR limits," *IEEE Trans. Smart Grid*, vol. 11, no. 1, pp. 301–311, Jan. 2020.
[20] J.-H. Liu and C.-C. Chu, "Wide-area measurement-based voltage stability indicators by modified coupled single-port models," *IEEE Trans. Power Syst.*, vol. 29, no. 2, pp. 756–764, Mar. 2014.
[21] B. Cui and Z. Wang, "Voltage stability assessment based on improved coupled single-port method," *IET Gener., Transmiss. Distrib.*, vol. 11, no. 10, pp. 2703–2711, Jul. 2017.
[22] Q. Sun, H. Cheng, and Y. Song, "Bi-objective reactive power reserve optimization to coordinate long- and short-term voltage stability," *IEEE Access*, vol. 6, pp. 13057–13065, 2018.
[23] Y. Wang, C. Lu, and X. Zhang, "Applicability comparison of different algorithms for ambient signal based load model parameter identification," *Int. J. Electr. Power Energy Syst.*, vol. 111, pp. 382–389, Oct. 2019.
[24] M. W. Asres, A. A. Girmay, C. Camarda, and G. T. Tesfamariam, "Non-intrusive load composition estimation from aggregate ZIP load models using machine learning," *Int. J. Electr. Power Energy Syst.*, vol. 105, pp. 191–200, Feb. 2019.
[25] R. D. Zimmerman and C. E. Murillo-Sánchez. (2016). *MATPOWER*. [Online]. Available: http://www.pserc.cornell.edu/matpower/
[26] R. D. Zimmerman, C. E. Murillo-Sanchez, and R. J. Thomas, "MATPOWER: Steady-state operations, planning, and analysis tools for power systems research and education," *IEEE Trans. Power Syst.*, vol. 26, no. 1, pp. 12–19, Feb. 2011.

PINGFENG YE (Student Member, IEEE) received the B.E. degree in electrical engineering from Shandong University, Jinan, China, in 2010, where he is currently pursuing the Ph.D. degree. His research interests include power system operation and control, and reactive power optimization.

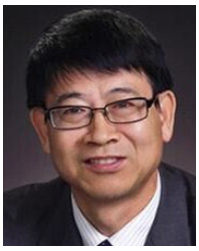

XUESHAN HAN received the B.E. and M.S. degrees in electrical engineering from Northeast Dianli University, Jilin, China, in 1984 and 1989, respectively, and the Ph.D. degree in electrical engineering from the Harbin Institute of Technology, Harbin, China, in 1994. From October 1998 to October 2000, he conducted postdoctoral research at Nanyang Technological University, Singapore. He is currently a Full Professor of electrical engineering with Shandong University. In recent 15 years, he leads a research group to develop the dispatch theory of modern power systems at Shandong University. He has published more than 200 academic articles. His research interests include power system operation and control, power system reliability assessment, and power economics.

MING YANG (Senior Member, IEEE) received the B.Eng. and Ph.D. degrees in electrical engineering from Shandong University, Jinan, China, in 2003 and 2009, respectively. From October 2006 to October 2007, he was an Exchange Ph.D. Student with the Energy System Research Center, The University of Texas at Arlington, Arlington, TX, USA. From July 2009 to July 2011, he conducted postdoctoral research with the School of Mathematics, Shandong University. From November 2015 to October 2016, he was a Visiting Scholar with the Energy Systems Division, Argonne National Laboratory, Argonne, IL, USA. He is currently a Professor with Shandong University. His research interest includes power system optimal operation and control. He is also an Associate Editor of the IEEE TRANSACTIONS ON INDUSTRY APPLICATIONS and *IET Renewable Power Generation*. He is also an Editor of *Protection and Control of Modern Power Systems*.

YUMIN ZHANG (Member, IEEE) received the Ph.D. degree from Shandong University, Jinan, China, in 2019. She is currently a Lecturer with the College of Electrical Engineering and Automation, Shandong University of Science and Technology, Qingdao, Shandong, China. Her research interests include power system operation and control, electricity market, and demand response.

YOUNAN PEI received the B.E. degree in electrical engineering from Shandong University, Jinan, China, in 2010, where he is currently pursuing the Ph.D. degree. His research interests include power system operation and control and optimal transmission switching.

XUAN ZHANG (Student Member, IEEE) was born in Jiangsu, China, in 1995. He joined the Shandong University of Science and Technology, in 2019, where he is currently pursuing the M.S. degree in electrical engineering.

His research interests include power system operation control and artificial intelligence techniques.